ISSN 1392-2114 ULTRAGARSAS, Nr.1(58). 2006.

Power amplifier for ultrasonic transducer excitation

L. Svilainis, G. Motiejūnas

Signal processing department, Kaunas University o f Technology,
Studentu str. 50, LT-51368 Kaunas, Lithuania, tel. +370 37 300532, E-mail.:svilnis@ktu.lt

Abstract

Design of the power amplifier for ultrasonic transducer excitation is presented. We assumed that the amplifier output impedance will be significantly lower than the transducer input impedance. Therefore we suggest to used the transformer as voltage step-up and impedance matching element. The transformer influence on the ultrasonic transducer bandwidth and the power transfer efficiency are analyzed using the Butterworth-Van Dyke transducer model. The transformer magnetizing and leakage inductance influence on a particular air coupled transducer are investigated by modeling and experimentally. The transformer application allows using the same carrier type (n-p-n bipolar or n-channel MOSFET) active elements in a push-pull configuration at the amplifier output stage. The commercially available relatively low voltage MOSFET is suggested. Two types of MOSFET transistors are investigated. The resulting amplifier performance has been investigated. The 50 kHz to 3 MHz bandwidth is obtained for the suggested amplifier configuration. The distortion and efficiency performance are investigated experimentally and using the P-SPICE modeling over various input signals ranges. The total harmonic distortion of 4% using 3 kΩ load and 400Vp-p 1MHz frequency signal is achieved. The investigation indicates the ability to use such a power amplifier for arbitrary waveform or high power continuous waveform excitation of ultrasonic transducers.

Keywords: high voltage power amplifier, arbitrary waveform excitation, ultrasonics transducer excitation

Introduction

The high ultrasonic transducer excitation voltage permits improvement of the signal to noise ratio (SNR) [1,2]. Usually air coupled transducers require high excitation voltages. This is because of large acoustic impedance mismatch between air and transducer and attenuation in air. If a solid body air coupled inspection is used, this adds additional mismatching interface, so the attenuation increases more. Therefore, a high power excitation becomes even more crucial. If same transducer is used for both the signal transmission and reception one is loosing the ability to operate the transducer at a serial resonance. Therefore the transducer input impedance is larger, so even higher excitation voltages are needed. The parasitic input capacitance of the ultrasonic transducer is clamping the power amplifier output, reducing the amplifier efficiency. In this paper we are analyzing the possibility to use the high turns ratio transformer in a power amplifier used for a high impedance ultrasonic transducer excitation. The aim is to get a high output voltage and a relatively wide power amplifier bandwidth. Air-coupled transducers operate up to 1-2 MHz. The lowest range is limited by 20-40 kHz, but nowadays there is a tendency to consider frequencies above 100 kHz. So we shall restrict our task to the 0.1-2 MHz frequency band.

The excitation

A power amplifier is the last stage used for the transducers excitation. The aim is to supply as much power as possible to the ultrasonic transducer. Because of high input impedance, the output voltage should be high, reaching the kilovolts region.

The ultrasonic transducer in a main resonance frequency region can be described using the Butterworth-Van Dyke (BVD) model [1]. This model (refer to Fig.1) describes the mechanical part (R_s, L_s, C_s) and the electrical part (the clamping capacitor C_0) of the transducer.

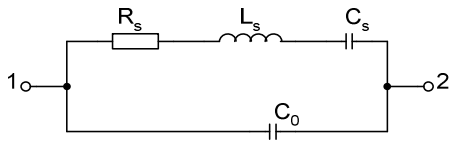

Fig. 1. **Butterworth-Van Dyke transducer model**

The losses described by R_s, can be split:

$$R_S = R_0 + R_{xm}, \tag{1}$$

where R_0 describes the dielectric losses in piezoceramic material and R_{xm} the acoustic emission into medium. Assuming R_{xm} is the largest part, the power supplied to R_s can be considered as the transducer acoustic efficiency measure.

The derived ultrasonic transducer input impedance is given by:

$$Z_S = \frac{\left(R_S + j\omega L_S + \frac{1}{j\omega C_S}\right)\cdot\frac{1}{j\omega C_0}}{R_S + j\omega L_S + \frac{1}{j\omega C_S} + \frac{1}{j\omega C_0}}. \tag{2}$$

From Eq.2 we get the resonance frequencies for the serial

$$\omega_n = \frac{1}{\sqrt{L_S C_S}}, \tag{3}$$

and the parallel resonance:

$$\omega_l = \frac{1}{\sqrt{L_S \frac{C_S C_0}{C_S + C_0}}}. \tag{4}$$

Due to the clamping effect of C_0 the amplifier driving efficiency is reduced. This results in unnecessary heating of the amplifier stages. In radio frequency (RF) applications the generator power, supplied to a load, efficiency is optimal when the generator impedance is the complex conjugate of the load [3]. By applying the passive matching circuit the parasitic input capacitance of the

ultrasonic transducer is absorbed into matching circuit or resonated out [4]. When resonating out the load parallel capacitance, the parallel inductance can be used. This fact is especially interesting when matching transformer is used to match the real part of the amplifier output low impedance to the high impedance ultrasonic transducer [5]. The idea is that the transformer magnetizing inductance might be usefully exploited not only for ensuring the transformer bandwidth, but also to reduce the ultrasonic transducer clamping capacitor effect.

The air coupled ultrasonic transducer was used for investigation. The transducer BVD model parameters are: R_s=3.3 kΩ, L_s=24.2 mH, C_s=26 pF, C_0=120 pF. The series resonance frequency is 205 kHz; the parallel resonance is at 230 kHz. The aim of the modeling was to investigate the transformer inductance influence on transfer efficiency and the bandwidth. Since in the BVD model the series resonant resistance R_s is presenting the power transmission to the media, the power delivered to R_s was used for bandwidth measurements and the transfer efficiency evaluation. The transducer input impedance, expected at the series resonance should be approximately 3.3 kΩ, clamped by C_0. We have used the generator output impedance equal to this value.

As indicated in [1], the additional inductor should resonate with the clamping capacitor C_0. The parallel inductance calculated to be 5 mH. The modeling results for an acoustic emission power delivery over a frequency range are presented in Fig.2.

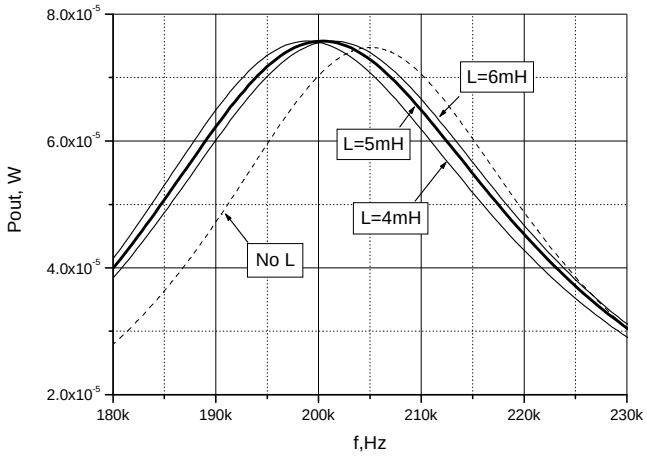

Fig. 2**. Acoustic emission power frequency response**

Three inductance values were investigated – the +20% and -20% deviations from the calculated value in order to evaluate the influence of the inductance accuracy. Analyzing the acoustic power delivered to the final load – R_s, one can see that the parallel inductance application just slightly shifts the maximum towards the lower frequencies. The signal level is not significantly changed. It is interesting to investigate how much the efficiency is altered by application of the inductance. The generator power transfer efficiency was calculated as the ratio of the power P_{Rs} delivered to R_s and the power P_g taken from the signal generator:

$$\eta_{tr} = \frac{P_{Rs}}{P_g}. \qquad (3)$$

The modeling results the generator power transfer efficiency are presented in Fig.3.

It is seen from the results above that efficiency for the transducer without the parallel inductance is higher at the frequencies above the series resonance. This is due to the input impedance rising when approaching the parallel resonance, but the efficiency for a transducer with the parallel inductance is stable over a frequency range.

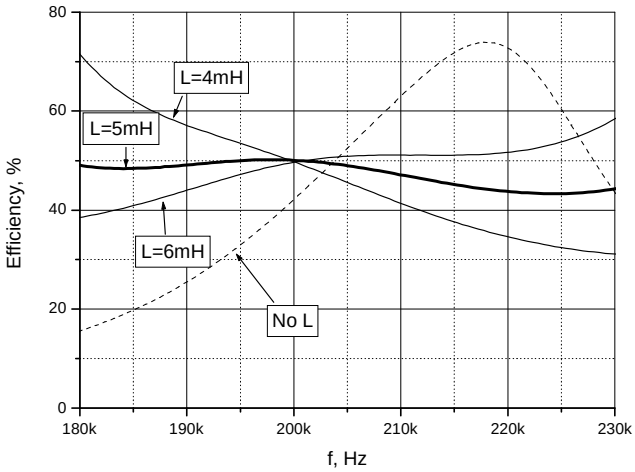

Fig. 3**. The generator power transfer efficiency**

The same results have been obtained when 1:1 turns ratio and the same magnetizing inductance transformer have been used to drive the transducer.

In the further investigation we have used the transformer with turns ratio 1:*n*. The secondary winding, driving the transducer magnetizing inductance was kept 5mH. The generator output impedance was 3.3 kΩ for turns ratio 1:1. In the case of 1: *n* ratio the impedance was reduced by n^2.

The results for the acoustic emission power frequency response when 1:*n* turns ratio transformer is used, are presented in Fig.4.

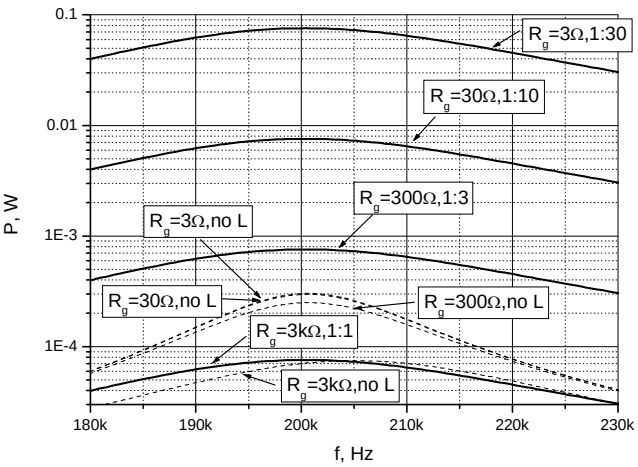

Fig. 4**. Acoustic emission power at various turns ratios**

We would like to point out that the vertical scale is logarithmic. This is because the variation for the transformer coupled case is very large – the power delivered increases by n^2. The case when no transformer is used and just the same output impedance generator is applied does not vary so significantly. When generator

output impedance is 10 times lower than the load lowest value, there is virtually no signal increase when the generator output impedance is reduced further.

The modeling results for the generator power transfer efficiency when the transformer coupling is used are presented in Fig.5.

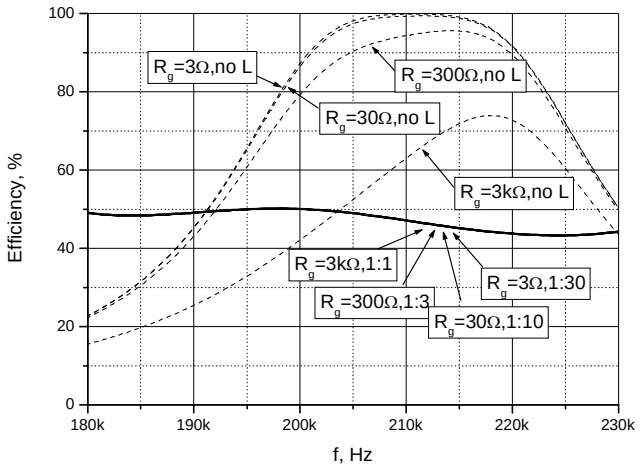

Fig. 5**. Generator power transfer efficiency at various turns ratios**

It should be noted that efficiency for all transformer coupled cases is the same. For reduced generator output impedance efficiency, the bandwidth is increased, but the acoustic power delivered to the transducer is not altered significantly. This can be seen in Fig.6 where all analyzed cases are presented. Note that all transformer coupling cases do not differ. The reason is that a linear, lossless transformer model is used. If transformer losses and parasitic parameters were taken into an account, then the cases would be different.

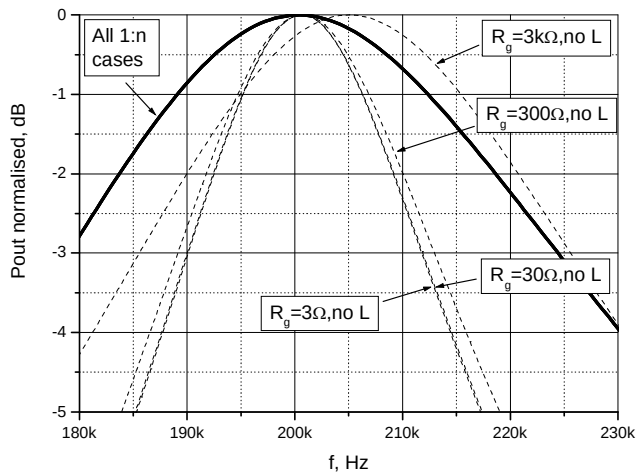

Fig. 6**. Normalized acoustic emission power**

From the presented investigation we see that there is no voltage increase due to the inductance resonant effect. It was indicated by Kažys in [3] that decision when to use the additional inductance in series or in parallel can be obtained from the transfer coefficient. For the serial case

$$K_s = \frac{\rho / R_g}{1 + R / R_g}, \qquad (7)$$

where ρ is the characteristic impedance of the resonant load.

For the parallel case:

$$K_p = \frac{1}{1 + R \cdot R_g / \rho^2}. \qquad (8)$$

From Eq. 7 and 8 it is seen that in the case $K_s > K_p$, when $\rho > R_g$ and the opposite, $K_s < K_p$, when $\rho < R_g$. For $\rho = R_g$ both solutions are equivalent. If we are matching the impedance, the this case should be analyzed.

It is interesting to analyze what effect on the amplifier performance will be caused by the transformer leakage inductance. Or, additional inductance can be added to mask the capacitor clamping effect or alter the bandwidth. Modeling and the experimental investigation have been performed with just the single inductor value – 4.7 mH. The resulting voltage on the resistance R_s is presenting the power transmission to the medium (refer to Fig.7).

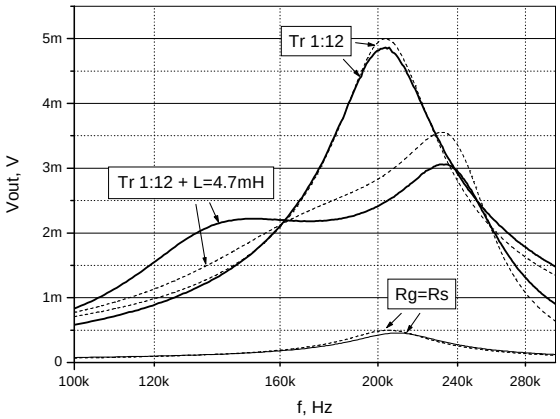

Fig. 7**. Serial inductance influence on voltage on R_s**

It can be seen that if a moderate step-up ratio 1:12 transformer is used, there is an ability to increase the bandwidth at some expence of a reduced signal level. This is clearly seen in Fig.8.

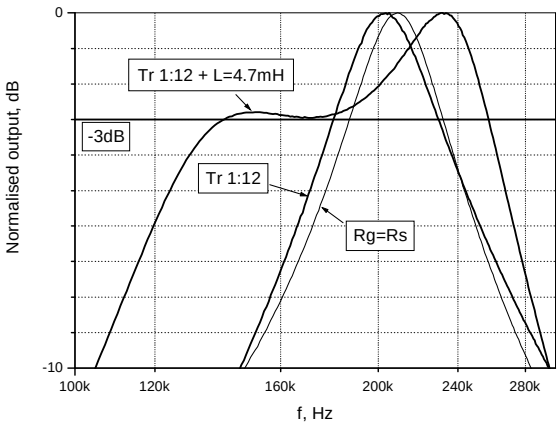

Fig. 8**. Serial inductance influence on normalized emission power**

The achievable bandwidth Δf can be calculated as [1]:

$$\frac{2\Delta f}{f} \cong \frac{1}{\sqrt{r}}, \qquad (5)$$

where

$$r = \frac{\pi^2}{8}\left(\frac{1-k_t^2}{k_t^2}\right), \qquad (6)$$

Here k_t is the electromechanical coupling coefficient of a piezoelectric transducer. The equations indicate that the bandwidth expansion is possible through reduction of the electromechanical coefficient k_t. But this solution has a drawback – the sensitivity will decrease.

The modified input impedance real and imaginary part graphs are presented in Fig.9.

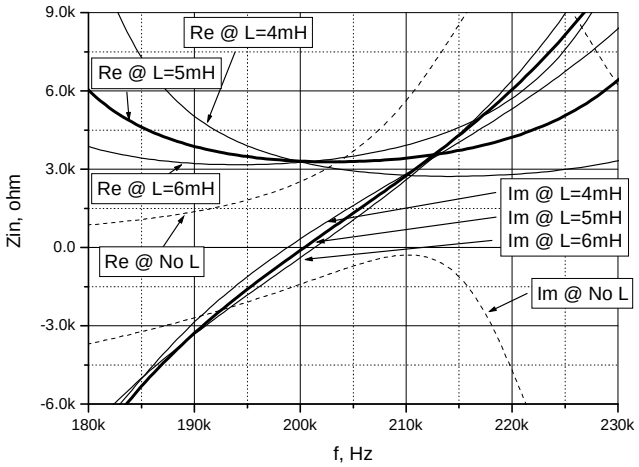

Fig. 9**. Parallel inductance influence on the input impedance**

The investigation has revealed that transformer coupling seems the attractive solution for a low impedance signal source matching into a high impedance transducer. For the particular transducer the input impedance is about 3kΩ, therefore the design of a power amplifier should be directed for.

The power amplifier design

The application of the transformer as an impedance matching element allows considering the push-pull B class amplifier as an amplifier output stage [6]. Push-pull transistors operate at collector/drain stress voltages of twice the supply voltage. The symmetrical power delivery and the ability to use same carrier type (n-p-n bipolar or n-channel MOSFET) active elements make it very attractive in an ultrasonic transducer excitation amplifier. At low input voltages the push-pull is practical due a smaller size and a higher output power [7]. Push-pull delivers the power to the load on both halves of the input cycle. The transformer must have a center tapped primary. Half of each winding is used alternatively with the input cycle. The transistors are operated at a moderate DC bias level, which allows expecting a higher efficiency and a lower output impedance. Power levels in excess of 1kVA can be achieved with the push-pull topology. Therefore, we shall favor this topology the over single-sided drive [7] or a purely active amplifier stage [8]. The circuit operation topology is presented in Fig.10.

We decided to use 1:30 turns ratio transformer. The high step-up ratio allows using low power supply voltages. Thanks to a low power supply voltage, low voltage transistors can be used. At low voltages MOSFET transistors have advantage over bipolar – their gain and the channel conductivity are much higher. The relatively low operation frequencies allow using cheap MOSFET transistors used in switching applications. We have picked up two candidates for investigation. Their parameters are presented in Table 1.

The driving circuit has +/- 12V power supply. Its output voltage swing 20V p-p is far than enough to drive the MOSFET gate. The driving circuit gain 5 times is sufficient to be driven from a low voltage external signal source. The current feedback amplifiers AD8016 have been used. These are capable of 1000V/μs slew rate and 600mA output current, which might be needed to drive the MOSFET gate charge.

Table 1. **Candidate MOSFET parameters**

Parameter	IRF510	IRFZ34N
V_{DS} max, V	100	55
I_D max, A	5.6	29
P_D max, W	43	68
$Q_{g(TOT)}$ max, *nC*	30	34
C_{ISS},pF	135	700
g_{fs} min, S	1.3	6.5

The current feedback amplifiers are prone to oscillate when loaded by a purely capacitive load. Therefore to reduce the gate ringing the output has external series resistors R_1 R_2 of 10Ω. In order to have the bias control separated from the driving circuit, AC coupling capacitors C_1 C_2 together with chokes L_1 L_2 are used.

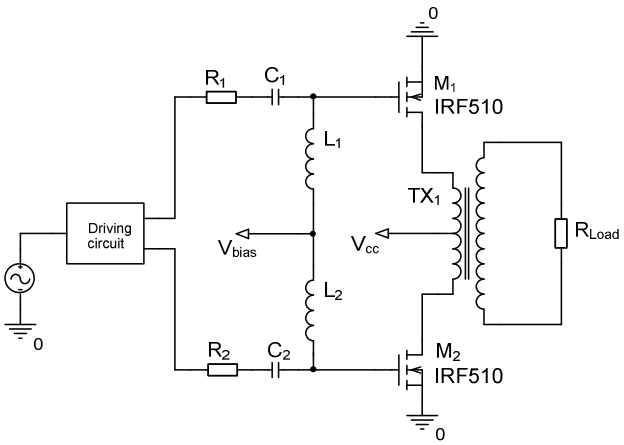

Fig. 10. **Push – pull power amplifier functional diagram**

Due to the requirement to have relatively low frequencies included in the passband, a high magnetizing inductance is required. Together with high the step-up ratio of the transformer, this sets the requirement to use the ferrite core. Ferrite has a DC resistivity in the crystallites. The NiZn ferrites a high volume resistivity up to 10^6 Ωm are suitable for frequencies over 1MHz due to a low permeability. We considered MnZn ferrites because of a higher permeability and higher induction levels. But the MnZn ferrites resistivity is lower - 0.1 to 10 Ωm. It must be kept in mind that the higher permeability usually means

the higher core losses. In our case it might cause the excessive core heating. Core influence on a coil is expressed by a complex permeability μ' (indicating the achievable inductance) and μ'' (indicating the core associated losses). Skipping the ferrite core analysis we just indicate that N27 material EPCOS toroidal ring core RM25 has been chosen [9]. The core parameters are summarized in Table 2.

Table 2. **Ferrite core parameters**

Parameter	Value
Material	N27 / 77
Initial permeability	2000
Power loss, mW	<580
A_L value, nH	2150
Suitable frequencies, MHz	0.001…2

The lowest passband frequency we require was set 100kHz. At this frequency the transformer primary winding magnetizing inductance impedance should be at least twice the output stage impedance. By using the driving circuit impedance and MOSFET transconductance the expected amplifier impedance is of 7.3 Ω and 1.5 Ω for IRF510 and IRFZ34N respectively. The required primary winding magnetizing inductance then should be about 7μH or 2μH. The two windings on the core chosen will give 8.6μH which we consider sufficient for both cases.

The performance investigation

The modeling of the chosen output stage using the IRF510 power MOSFETs has been performed. The schematic diagram used is presented Fig.11.

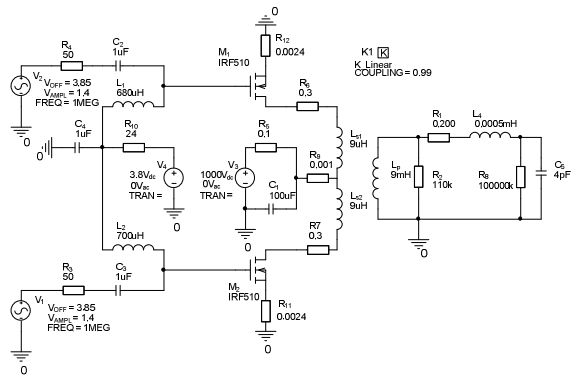

Fig. 11**. Circuit used for modeling**

Skipping all the iteration stages used in modeling we just present the harmonic distortion performance at 1MHz. The first four harmonics are presented in Fig.12 together with the results of the experimental investigation.

A low power supply voltage of 7V was used in order to keep the power consumption down. After closer examination it can be seen that at higher excitation voltages the first harmonic starts to decrease. This is due to a reduced power supply and increased distortion at higher power levels.

It was interesting to find out what output levels can be achieved. This has been investigated experimentally for both IRF510 and IRFZ34N power MOSFETs (Fig.13).

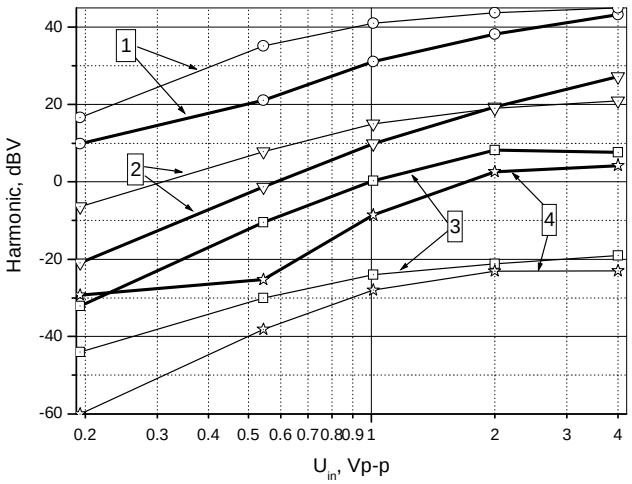

Fig. 12**. Output signal harmonics vs input signal; modeling (thin lines) and experiment (solid) results**

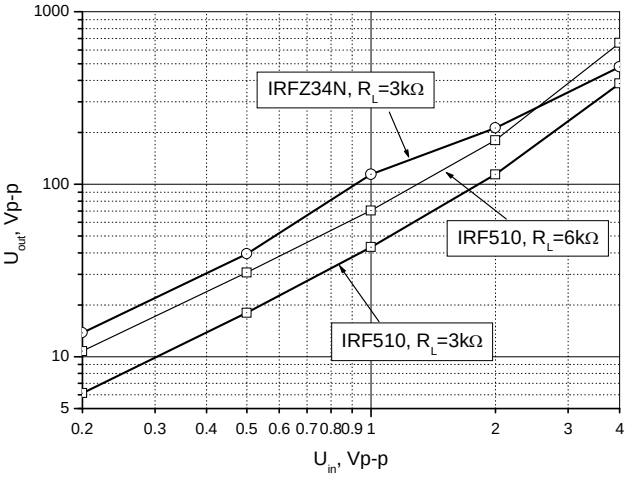

Fig. 13**. Output voltage versus the input voltage**

It can be seen that the response is linear at output voltages up to 200V. The +7V power supply in this region was sufficient. In the upper voltages region the the supply voltage was not sufficient, so the signal was clipped. Therefore the power supply has been increased up to 20V for IRF510 MOSFET amplifier configuration. The IRFZ34N configuration power supply was kept the same. Probably this has caused discrepancies in a higher voltages region.

The achieved power supply conversion efficiency versus the input signal is presented in Fig.14.

Again, the power supply limitation influence is seen in a higher voltages region. The expected power efficiency in practice will be lower, since regulation of a power supply voltage is not justified in practical applications. Assuming that this power amplifier will be used in a pulsed excitation mode, using an arbitrary waveform or a continuous wave (CW) burst, such efficiency should be a sufficient. Otherwise MOSFETs and especially IRFZ34N should be supplied with sufficient heatsink. The current configuration has just light aluminum plate as a heatsink, which is applied because of both transistors temperature equalization, but not for cooling purposes. The output voltage rise associated with a total harmonic distortion (THD) also has been investigated experimentally for both MOSFETs. The results are presented in Fig.15.

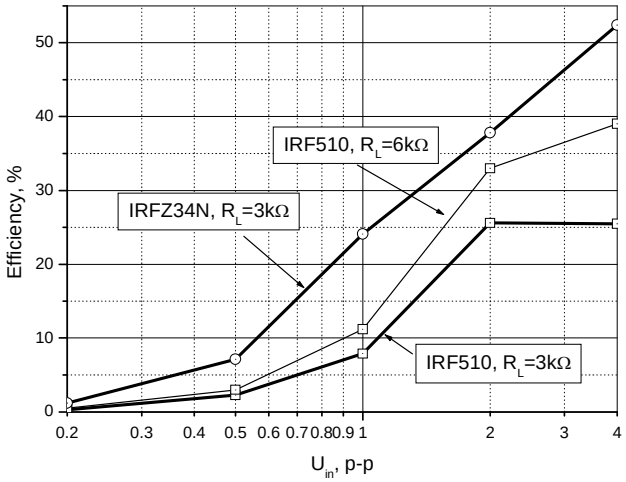

Fig. 14**. Efficiency versus input voltage**

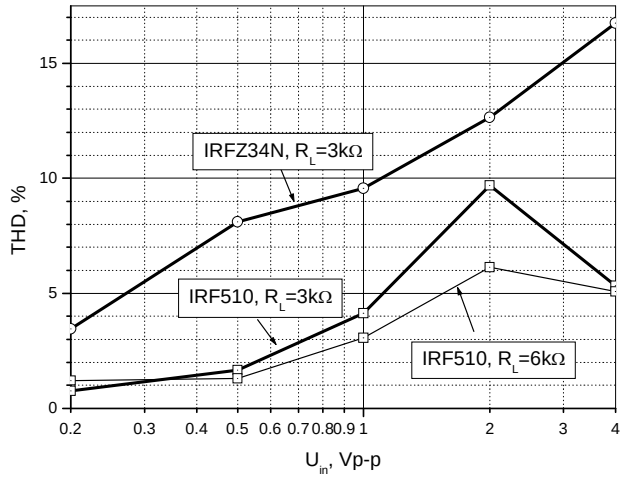

Fig. 15**. Total harmonic distortion versus input voltage**

THD is generated when a sine wave magnetic field (current) induces a non-sinusoidal flux density due to a non linear relation between the field and the flux in the ferrite core of a transformer. Some distortion occurs at low flux densities. This can be seen in Fig.12 and 15. When the field strength is increased, the flux density increases more than linearly with the field, which results in a distorted sinusoidal voltage shape. The other type of distortion appears at high signal levels when the flux density comes close to its saturation level. A further increase in a current (field) cannot result in a linear increase of the flux any more, which gives the distorted voltage shape. This type of THD is seen at the right side of Fig.15. The THD reduction at higher voltages for IRF510 configuration can be explained by a power supply increase, causing a more linear MOSFET operation. The IRFZ34N configuration is possessing a higher distortion due to higher transconductance level and absence of the negative feedback.

The graphs in Fig.16 picture the amplifier output impedance variation over the input signal amplitude range.

The amplifier output impedance was investigated by using the open circuit measurement results together with the data obtained at the load condition. The impedance is more or less stable over the voltage range for IRF510 configuration. The dip at the 2V input is caused by clipping - the active element resulting conductivity has

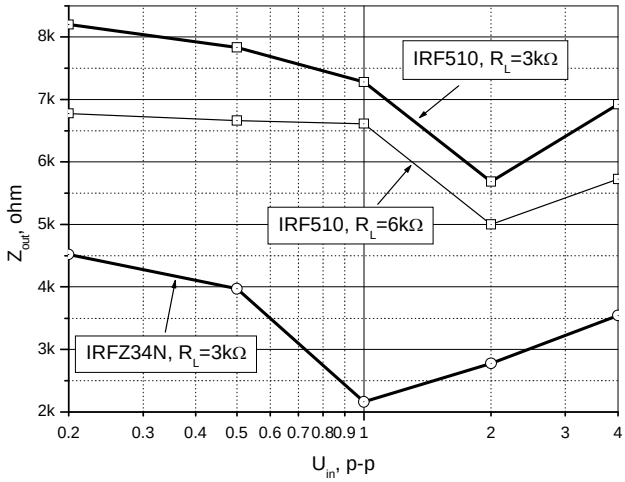

Fig. 16**. Amplifier output impedance versus input voltage**

been increased. It should be noted that IRFZ34N power MOSFETs due to its higher transconductance is not that stable as IRF510. Due to this, the impedance variation is quite large. In addition to impedance stability problems IRFZ34N also features instability in biasing and bandwidth over temperature. If used in a pulsed mode it might be the candidate for a power amplifier. Otherwise, the additional bias control techniques should be used for this MOSFET.

The power amplifier initially was designed for 100kHz to 2 MHz frequency region. Experimental investigation has been carried out to evaluate its frequency performance. The normalized output response over 50 kHz to 3 MHz frequency range is presented in Fig.17 (for IRF510) and Fig.18 (for IRFZ34N).

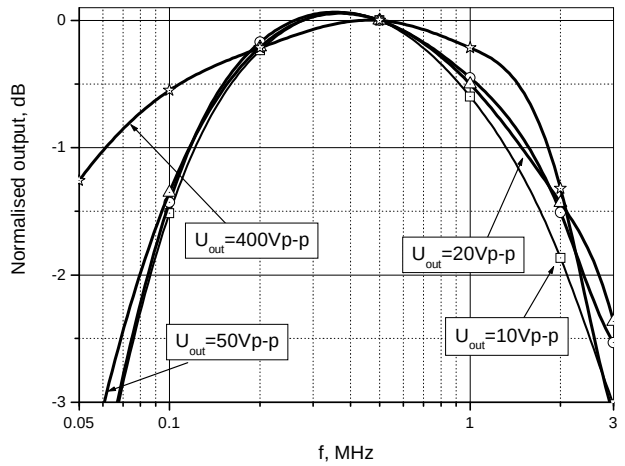

Fig. 17**. Frequency response for IRF510 configuration**

It can be seen that IRF510 is perfectly managing the desired bandwidth. It was expected to have a much wider frequency response, but due to high step-up ratio leakage inductance was high, reducing the response in a high frequency region. The expansion to lower frequencies is possible if higher magnetizing inductance values are used. For the current design the 1:30 turns ratio is at the core fill-factor limit. If lower turns ratio is used, other output impedances are available. The resulting output voltages range will be reduced. This can be easily compensated by raising the power supply voltage – IRF510 has 100V drain-source breakdown voltage.

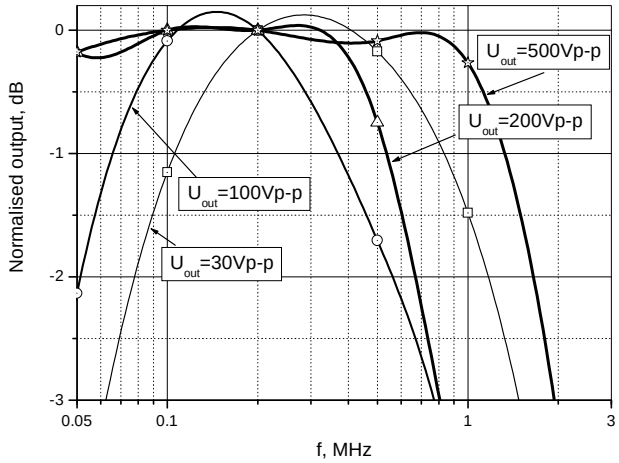

Fig. 18**. Frequency response for IRFZ34N configuration**

Despite the lower output impedance seen in Fig.16, the IRFZ34N has a narrower bandwidth. The explanation is a higher gain and a higher input capacitance. If a lower driving circuit output impedance is used, the bandwidth could be expanded. Increasing the bias current for IRFZ34N, a much lower output impedance or a higher output voltage can be achieved, but in such case the amplifier is prone to oscillate, saturate of simply burn down. Therefore, special precautions on biasing and temperature stabilization should be used then.

Conclusions

Assuming that the transducer input impedance is higher than the amplifier output we suggested using the transformer as a voltage step-up and impedance matching element. The transformer appearance at the amplifier output allows designing the B class push-pull amplifier output. The high transformer step-up ratio allows use low power supply voltages. Thanks to this low voltage MOSFETs can be used, which are quite cheap. The distortion and bandwidth performance indicate the ability to use such a power amplifier for the low frequency (100kHz to 2MHz) ultrasonic transducer excitation, using an arbitrary waveform external source. The moderate power supply usage efficiency also allows excitation by a high power continuous waveform in the indicated frequency range.

References

1. **Domarkas V., Kažys R.-J.** Piezoelectric transducers for measuring devices. Vilnius: Mintis. 1975. P. 255.
2. **Ramos A., Emeteriao J. L. S.** Improvement in transient piezoelectric responses of NDE transceivers using selective damping and tuning networks IEEE transactions on ultrasonics ferroelectrics and frequency control. 2000. Vol 47. No 4. P. 826-835
3. **Cripps S.** Advanced techniques in RF power amplifier design. Artech House Inc. 2002. P.259.
4. **Besser L.** Practical RF circuit design for modern wireless systems. Artech House Inc. 2003. P.233.
5. **Kauczor C., Fr6hleke N.** Inverter topologies for ultrasonic piezoelectric transducers with high mechanical Q-factor 35th Annual IEEE Power Electronics Specialists Conference, Aacken, Germany. 2004. P.2736-2741.
6. **Ishikawa J., Mizutani Y., Suzuki T., Ikeda H. and Yoshida H.** High-frequency drive-power and frequency control for ultrasonic transducer operating at 3 MHz. IEEE Industry Applications Society Annual Meeting, Louisiana. 1997. P.900-905.
7. **Mizutani Y., Suzuki T., Ikeda H. and Yoshida H.** Power maximizing of ultrasonic transducer driven by MOS-FET inverter operating at 1 MHz Proceedings of the IEEE IECON 22nd International Conference. 1996. P.983-986.
8. **Brown J. A., Lockwood G. R.** A low-cost, high-performance pulse generator for ultrasound imaging. IEEE transactions on ultrasonics ferroelectrics and frequency control. 2002. Vol 49. No 6. P. 848-851.
9. SIFERRIT Materials. EPCOS AG Marketing Communications, Munich, Germany. 2001. P.31-106.

L. Svilainis, G. Motiejūnas

Stiprintuvas ultragarsiniams keitikliams žadinti

Reziumė

Aptariamas galios stiprintuvo ultragarsiniams keitikliams žadinti projektavimas. Tarta, kad stiprintuvo išėjimo impedansas gerokai didesnis už ultragarsinio keitiklio įėjimo impedansą. Todėl siūloma naudoti transformatorių kaip įtampos sukėlimo ir apkrovos įėjimo impedanso derinimo elementą. Transformatoriaus įtaka ultragarsinio keitiklio juostai ir galios stiprintuvo efektyvumui analizuota naudojant Butterwortho ir Van Dyke‘o keitiklio modelį. Modeliuojant ir eksperimentiniais tyrimais aiškintasi transformatoriaus išėjimo ir nuotėkio induktyvumų įtaka konkrečiam ore dirbančiam keitikliui. Transformatorius leidžia stiprintuvo išėjimo laipsnyje naudoti to paties laidumo (n-p-n bipolinį ar n-kanalį MOSFET) aktyviuosius elementus. Pasiūlyta naudoti santykiškai žemos įtampos MOSFET tranzistorius. Nagrinėtas dviejų MOSFET tranzistorių tipų tinkamumas. Tirti suprojektuoto stiprintuvo parametrai. Siūlomai stiprintuvo konfigūracijai gauta nuo 50 kHz iki 3 MHz pralaidos juosta. Naudojant įvairius įėjimo signalo lygius, tirtas stiprintuvo efektyvumas ir iškraipymų lygis. Pasitelktas modeliavimas P-SPICE paketu ir eksperimentiniai tyrimai. Netiesinių iškraipymų koeficientas esant 3 kΩ apkrovos varžai ir 400Vp-p. 1 MHz siekia 4 %. Analizė parodė tokio stiprintuvo tinkamumą ultragarsiniams keitikliams žadinti laisvai pasirinktos formos arba didelės galios harmoniniais signalais.

Pateikta spaudai 2006 03 22

DOI: 10.5755/j01.u.58.1.16970